# Bound H Dibaryon in Flavor SU(3) Limit of Lattice QCD



doi: 10.1103/PhysRevLett.106.162002

# Bound $H$ Dibaryon in Flavor SU(3) Limit of Lattice QCD

Takashi Inoue,[1] Noriyoshi Ishii,[2] Sinya Aoki,[2,3] Takumi Doi,[3] Tetsuo Hatsuda,[4,5] Yoichi Ikeda,[6] Keiko Murano,[7] Hidekatsu Nemura,[8] and Kenji Sasaki[3]

(HAL QCD Collaboration)

[1]*Nihon University, College of Bioresource Sciences, Fujisawa 252-0880, Japan*
[2]*Center for Computational Sciences, University of Tsukuba, Tsukuba 305-8577, Japan*
[3]*Graduate School of Pure and Applied Sciences, University of Tsukuba, Tsukuba 305-8571, Japan*
[4]*Department of Physics, The University of Tokyo, Tokyo 113-0033, Japan*
[5]*IPMU, The University of Tokyo, Kashiwa 277-8583, Japan*
[6]*Nishina Center for Accelerator-Based Science, Institute for Physical and Chemical Research (RIKEN), Wako 351-0198, Japan*
[7]*High Energy Accelerator Research Organization (KEK), Tsukuba 305-0801, Japan*
[8]*Department of Physics, Tohoku University, Sendai 980-8578, Japan*
(Received 10 January 2011; published 20 April 2011)

The flavor-singlet $H$ dibaryon, which has strangeness $-2$ and baryon number 2, is studied by the approach recently developed for the baryon-baryon interactions in lattice QCD. The flavor-singlet central potential is derived from the spatial and imaginary-time dependence of the Nambu-Bethe-Salpeter wave function measured in $N_f = 3$ full QCD simulations with the lattice size of $L \simeq 2, 3, 4$ fm. The potential is found to be insensitive to the volume, and it leads to a bound $H$ dibaryon with the binding energy of 30–40 MeV for the pseudoscalar meson mass of 673–1015 MeV.

DOI: 10.1103/PhysRevLett.106.162002 PACS numbers: 12.38.Gc, 13.75.Ev, 14.20.Pt

Search for dibaryons is one of the most challenging theoretical and experimental problems in the physics of strong interaction and quantum chromodynamics (QCD). In the nonstrange sector, only one dibaryon, the deuteron, is known experimentally. In the strange sector, on the other hand, it is still unclear whether there are bound dibaryons or dibaryon resonances. Among others, the flavor-singlet state ($uuddss$), the $H$ dibaryon, has been suggested to be the most promising candidate [1]. The $H$ may also be a doorway to strange matter and to exotic hypernuclei [2]. Although deeply bound $H$ with the binding energy $B_H > 7$ MeV from the $\Lambda\Lambda$ threshold has been ruled out by the discovery of the double $\Lambda$ nuclei, ${}^{6}_{\Lambda\Lambda}$He [3], there still remains a possibility of a shallow bound state or a resonance in this channel [4].

While several lattice calculations on $H$ have been reported as reviewed in [5] (see also recent works [6–8]), there is a serious problem in studying dibaryons on the lattice: To accommodate two baryons inside the lattice volume, the spatial lattice size $L$ should be large enough. Once $L$ becomes large, however, energy levels of two baryons become dense, so that quite a large imaginary time $t$ is required to make clear isolation of the ground state from the excited states. All the previous works on dibaryons more or less face this issue.

The purpose of this Letter is to shed a new light on the $H$ dibaryon by extending the lattice approach recently proposed by the present authors [7,9]. Our starting point is the baryon-baryon potential obtained from the Nambu-Bethe-Salpeter (NBS) amplitude measured on the lattice [9]. Such a potential together with the NBS amplitude can be shown to satisfy the Schrödinger-type equation and to reproduce the correct phase shifts at low energies. It was found on the lattice in the flavor SU(3) limit [7] that, while the celebrated repulsive core of the potential appears in the nucleon-nucleon (NN) channels, the ''attractive core'' emerges in the $H$-dibaryon channel. These features at the short range part of the potential are essentially dictated by the Pauli exclusion principle in the quark level: Six quarks residing at the same spatial point is partially forbidden by the quark Pauli effect in the NN channels, which belong to the flavor 27-plet or 10*-plet, while the flavor-singlet six quarks do not suffer from the Pauli effect [10].

The approach based on the baryon-baryon potential has several advantages. In particular, it can be used not only to reduce the finite volume artifact but also to avoid the problem of contaminations from excited states, as will be explained later. In this Letter, to capture essential features of the $H$ dibaryon without being disturbed by the quark mass differences, we consider the flavor SU(3) limit where all $u$, $d$, and $s$ quarks have a common finite mass. This allows us to extract baryon-baryon potentials for irreducible flavor multiplets and to make the comparison among different flavor channels in a transparent manner.

We start with the NBS wave function [9] defined by

$$\phi_n(\vec{r}) = \langle 0|(BB)^{(\alpha)}(\vec{r}, 0)|W_n; \alpha\rangle, \quad (1)$$

 

where the state vector $|W_n;\alpha\rangle$ is a QCD eigenstate with the baryon number 2 (6 quark state) and energy $W_n$ in the flavor $\alpha$-plet. $(BB)^{(\alpha)}(\vec{r},t)=\sum_{i,j,\vec{x}}C_{ij}^{(\alpha)}B_i(\vec{x}+\vec{r},t)B_j(\vec{x},t)$ is a two-baryon operator with a relative distance $\vec{r}$ in $\alpha$-plet with $B_i$ being a one-baryon composite field operator in the flavor octet. The relation between two-baryon operators in the flavor basis and baryon basis is given by the SU(3) Clebsch-Gordan coefficients.

In the lattice QCD simulations, the above NBS wave function is extracted from the four point function as

$$\begin{aligned} G_4(\vec{r},t-t_0) &= \langle 0|(BB)^{(\alpha)}(\vec{r},t)\overline{(BB)}^{(\alpha)}(t_0)|0\rangle \\ &= \sum A_n\phi_n(\vec{r})e^{-W_n(t-t_0)}, \\ A_n &= \langle W_n;\alpha|\overline{(BB)}^{(\alpha)}|0\rangle. \end{aligned} \tag{2}$$

Here $\overline{(BB)}^{(\alpha)}(t_0)$ is a wall source operator at time $t_0$ to create two-baryon states in $\alpha$-plet, while $(BB)^{(\alpha)}(\vec{r},t)$ is the sink operator at time $t$ to annihilate the two-baryon states. Even if we choose $t-t_0$ moderately large so that the inelastic scatterings (e.g., the scattering with excited baryons and the scattering with meson production) do not contribute to $G_4$, there still remain elastic scattering states with low energy excitations due to the relative motion of the baryons. For example, with the baryon mass $M\simeq 2$ GeV in a finite box of $L=4$ fm, the noninteracting two-baryon system has $W_1-W_0\simeq(2\pi/L)^2/(2\mu)\simeq 50$ MeV, with the reduced mass $\mu=M/2$. This requires $t-t_0>10$ fm to achieve $1/10$ suppression of the first excited state $\phi_1(\vec{r})$ in $G_4(\vec{r},t-t_0)$. It is beyond most of the previous and current lattice simulations.

Our potential approach avoids the above problem in the following way: The two-body potential in low energy QCD dictates all the elastic scattering states $\phi_n(\vec{r},t)=\phi_n(\vec{r})e^{-(W_n-2M)t}$ simultaneously through the Schrödinger equation in the Euclidean space-time [9]. With the nonrelativistic approximation for $W_n$, it reads

$$H_0\phi_n(\vec{r},t)+\int d^3r' U(\vec{r},\vec{r}')\phi_n(\vec{r}',t)=-\frac{\partial}{\partial t}\phi_n(\vec{r},t), \tag{3}$$

where $H_0=-\nabla^2/(2\mu)$ and $U$ is a nonlocal and energy-independent potential. Since the above equation is linear in $\phi_n$, the linear combination such as $\phi(\vec{r},t)\equiv\sum_n A_n\phi_n(\vec{r},t)=G_4(\vec{r},t)/e^{-2Mt}$ also satisfies Eq. (3). We note that the derivative expansion of $U$ in terms of its nonlocality leads to $U(\vec{r},\vec{r}')=[V_C(r)+V_T(r)S_{12}+V_{LS}(r)\vec{L}\cdot\vec{S}+\cdots)\delta(\vec{r}-\vec{r}')$ [9], where $V_C$, $V_T$, and $V_{LS}$ are the central, tensor, and spin-orbit potentials, respectively, and dots stand for terms including the power of $\nabla$. It was shown in [11] that the leading order potentials without $\nabla$ dominate the potential at low energies. Thus, the relevant term in the spin-singlet channel, $V_C$, is obtained as

$$V_C(r)=\frac{[-H_0-(\partial/\partial t)]\phi(\vec{r},t)}{\phi(\vec{r},t)}. \tag{4}$$

In this way, one can extract the baryon-baryon potential without identifying each elastic state $\phi_n(\vec{r},t)$ as long as $t-t_0$ is so chosen that the inelastic scatterings are suppressed. Once we obtain the volume independent $V_C$, binding energies and scattering phase shifts in the infinite volume are obtained by solving the Schrödinger equation. In contrast to the conventional Lüscher's method [12], we do not calculate the energy shift of two hadrons at finite $L$ to access the observables at $L\to\infty$. Further theoretical details of this method will be given in a separate publication [13].

Let us now consider the interaction between flavor-octet baryons in the flavor SU(3) limit, for which two baryon states with a given angular momentum are labeled by the irreducible flavor multiplets as $\mathbf{8}\otimes\mathbf{8}=(\mathbf{27}\oplus\mathbf{8}_s\oplus\mathbf{1})_{\text{symmetric}}\oplus(\mathbf{10}^*\oplus\mathbf{10}\oplus\mathbf{8}_a)_{\text{antisymmetric}}$. Here "symmetric" and "antisymmetric" stand for the symmetry under the flavor exchange of two baryons. For the system in the orbital $S$ wave, the Pauli principle between two baryons imposes $\mathbf{27}$, $\mathbf{8}_s$, and $\mathbf{1}$ to be spin singlet ($^1S_0$) while $\mathbf{10}^*$, $\mathbf{10}$, and $\mathbf{8}_a$ to be spin triplet ($^3S_1$). Since different multiplets are independent in the flavor SU(3) limit, one can define the corresponding potentials as $V^{(\mathbf{27})}(r), V^{(\mathbf{8}_s)}(r), V^{(\mathbf{1})}(r)$ for $^1S_0$ and $V^{(\mathbf{10}^*)}(r), V^{(\mathbf{10})}(r), V^{(\mathbf{8}_a)}(r)$ for $^3S_1$. Hereafter, we focus on the flavor-singlet channel with

$$BB^{(1)}=-\sqrt{\frac{1}{8}}\Lambda\Lambda+\sqrt{\frac{3}{8}}\Sigma\Sigma+\sqrt{\frac{4}{8}}N\Xi, \tag{5}$$

where $\Lambda$, $\Sigma$, $N$, and $\Xi$ are the standard baryon operators with Lorentz structure, $[q(C\gamma_5)q]q$ [7].

In our dynamical lattice QCD simulations, we employ the renormalization group improved Iwasaki gauge action and the nonperturbatively $O(a)$ improved Wilson quark action. For $16^3\times 32$ lattice, we use the configuration set generated by CP-PACS and JLQCD Collaborations [14] at $\beta=1.83$. In addition, we generate gauge configurations with the same $\beta$ for $24^3\times 32$ and $32^3\times 32$ lattices, using the DDHMC/PHMC code [15]. Quark propagators are calculated for the spatial wall source at $t_0$ with the Dirichlet boundary condition in the temporal direction. The sink operator is projected to the $A_1^+$ representation of the cubic group, so that the NBS wave function is dominated by the $S$-wave component. For the time derivative, we adopt the symmetric difference on the lattice. Lattice parameters such as lattice spacing $a$, the hopping parameter $\kappa_{uds}$, the number of configurations $N_{\text{cfg}}$, together with the pseudoscalar meson mass $m_{\text{ps}}$ and the octet baryon mass $m_B$ are summarized in Table I for the $32^3\times 32$ lattice.

To check the qualitative consistency with previous works, we show in Fig. 1 the central potential in the

TABLE I. Summary of lattice parameters and hadron masses. The uncertainty of $a$ [14] is not reflected in hadron masses.

| $a$ (fm) | $L$ (fm) | $\kappa_{uds}$ | $m_{\rm ps}$ (MeV) | $m_B$ (MeV) | $N_{\rm cfg}$ |
|---|---|---|---|---|---|
| | | 0.13710 | 1015.0(6) | 2030(2) | 360 |
| 0.121(2) | 3.87 | 0.13760 | 836.5(5) | 1748(1) | 480 |
| | | 0.13800 | 672.9(7) | 1485(2) | 240 |

27-plet channel $V_C^{(27)}(r)$ obtained in three different lattice volumes with $L = 1.94, 2.90, 3.87$ fm at $m_{\rm ps} = 1015$ MeV and $(t - t_0)/a = 10$. This is the case corresponding to the NN potential in the $^1S_0$ channel. Compared with statistical errors, the $L$ dependence is found to be negligible. The $t$ dependence is also small as long as $(t - t_0)/a \geq 9$. Note that we do not need overall shift of the potential: it approaches zero automatically as $r$ increases. The figure shows a repulsive core at short distance surrounded by an attractive well at medium and long distances, which is qualitatively consistent with our previous results in quenched and full QCD simulations reviewed in [16].

Shown in Figs. 2(a) and 2(b) are the volume dependence and the quark mass dependence of the central potential in the flavor-singlet channel $V_C^{(1)}(r)$, respectively. In both figures, we take $(t - t_0)/a = 10$, and have checked that the potentials do not have appreciable change with respect to the choice of $t$. We find that the flavor-singlet potential has an "attractive core" and its range is well localized in space. Because of the latter property, we find no significant volume dependence of the potential within the statistical errors as seen in Fig. 2(a). We find that the long range part of the attraction tends to increase as the quark mass decreases [Fig. 2(b)].

We fit the resultant potential by the following analytic function composed of an attractive Gaussian core plus a long range (Yukawa)$^2$ attraction: $V(r) = b_1 e^{-b_2 r^2} + b_3(1 - e^{-b_4 r^2})(e^{-b_5 r}/r)^2$. With the five parameters, $b_1$–$b_5$, we can fit the function to the lattice results reasonably well with $\chi^2/\text{d.o.f.} \simeq 1$. The fitted result for $L = 3.87$ fm is shown by the dashed line in Fig. 2(a).

Finally, using the potential fitted by the function, we solve the Schrödinger equation in the infinite volume and obtain the energies and the wave functions for the present quark masses in the flavor SU(3) limit. It turns out that, in each quark mass, there is only one bound state with the binding energy of 30–40 MeV. In Fig. 3(a), the energy and the root-mean-square (rms) distance of the bound state are plotted in the case of $(t - t_0)/a = 9, 10, 11$ at $m_{\rm ps} = 673$ MeV and $L = 3.87$ fm, where errors are estimated by the jackknife method. Although the statistical error increases as $t$ increases, we observe small changes of central values, which will be included as the systematic errors in our final results. Figure 3(b) shows the energy and the rms distance of the bound state at each quark mass obtained from the potential with $L = 3.87$ fm and $(t - t_0)/a = 10$. Despite the fact that the potential has quark mass dependence, the resultant binding energies of the $H$ dibaryon are insensitive in the present range of the quark masses. This is due to the fact that the increase of the attraction toward the lighter quark mass is partially compensated by the increase of the kinetic energy for the lighter baryon mass. It is noted that there appears no bound state for the potential of the 27-plet channel in the present range of the quark masses.

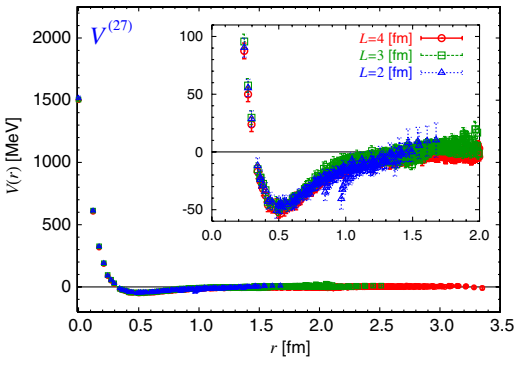


FIG. 1 (color online). Flavor 27-plet potential $V_C^{(27)}(r)$ obtained for lattice sizes $L = 1.94, 2.90, 3.87$ fm at $m_{\rm ps} = 1015$ MeV and $(t - t_0)/a = 10$. Inset shows a magnification.

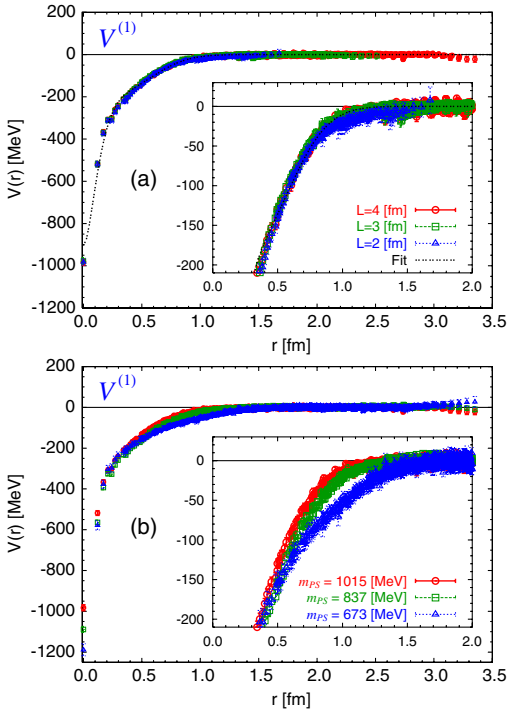


FIG. 2 (color online). Flavor-singlet potential $V_C^{(1)}(r)$ at $(t - t_0)/a = 10$. (a) Results for $L = 1.94, 2.90, 3.87$ fm at $m_{\rm ps} = 1015$ MeV. (b) Results for $L = 3.87$ fm at $m_{\rm ps} = 1015, 837, 673$ MeV. Insets show a magnification.

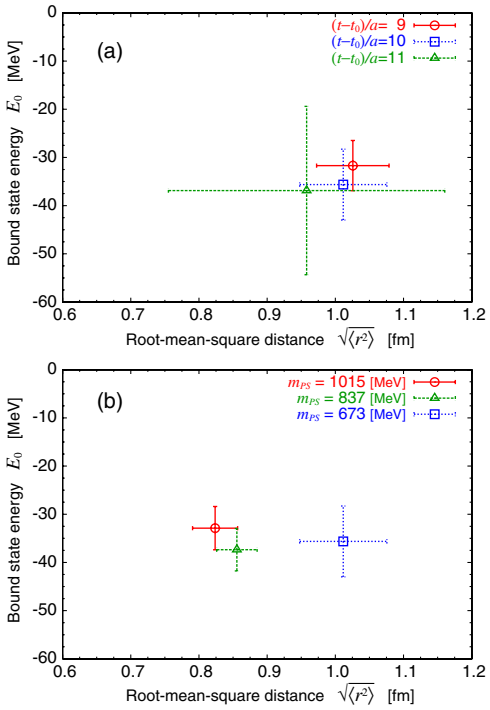


FIG. 3 (color online). Bound state energy $E_0 \equiv -\tilde{B}_H$ and the rms distance $\sqrt{\langle r^2\rangle}$ of the $H$ dibaryon obtained from the potential at $L = 3.87$ fm. (a) Imaginary-time dependence at $m_{\rm ps} = 673$ MeV. (b) Quark mass dependence at $(t - t_0)/a = 10$.

The final results of the binding energy in the SU(3) limit $\tilde{B}_H$ and the rms distance $\sqrt{\langle r^2\rangle}$ are given below, with statistical errors (first) and systematic errors from the $t$ dependence (second).

$$m_{\rm ps} = 1015 \text{ MeV } \tilde{B}_H = 32.9(4.5)(6.6) \text{ MeV}$$
$$\sqrt{\langle r^2\rangle} = 0.823(33)(40) \text{ fm},$$
$$m_{\rm ps} = 837 \text{ MeV } \tilde{B}_H = 37.4(4.4)(7.3) \text{ MeV}$$
$$\sqrt{\langle r^2\rangle} = 0.855(29)(61) \text{ fm},$$
$$m_{\rm ps} = 673 \text{ MeV } \tilde{B}_H = 35.6(7.4)(4.0) \text{ MeV}$$
$$\sqrt{\langle r^2\rangle} = 1.011(63)(68) \text{ fm}.$$

A less than 1% error from the choice for the fit function is not included here.

Since $\tilde{B}_H$ has the weak quark mass dependence, one may assume a similar binding energy is realized even with the realistic SU(3) breaking, where $\tilde{B}_H$ is interpreted as the binding energy from the average mass of two octet baryons in the $S = -2$ and $I = 0$ channel. Considering that the difference between this average and $2m_\Lambda$ is about the same amount as $\tilde{B}_H$, the $H$ dibaryon may appear as a weakly bound state or a resonant state near the $\Lambda\Lambda$ threshold, as mentioned in [7]. To make a definite conclusion on this point, however, we need $(2 + 1)$-flavor lattice QCD simulations with the $\Lambda\Lambda - N\Xi - \Sigma\Sigma$ coupled channel analysis as well as a careful study on the nonlocality of the potential. The extension of the method outlined in this Letter to this direction is in progress [17].

We thank authors and maintainers of CPS++ [18], K.-I. Ishikawa and PACS-CS Collaboration for DDHMC/PHMC code, and ILDG/JLDG [19] for providing configurations. This research is supported in part by MEXT Grant-in-Aid (20340047, 22540268), Scientific Research on Innovative Areas (20105001, 20105003, 21105515), Specially Promoted Research (13002001), and JSPS 21·5985, the Large Scale Simulation Program of KEK (09/10-24), and the collaborative interdisciplinary program at T2K-Tsukuba (10a-19).

[1] R. L. Jaffe, Phys. Rev. Lett. **38**, 195 (1977); **38**, 617 (1977); Reviewed in T. Sakai, K. Shimizu, and K. Yazaki, Prog. Theor. Phys. Suppl. **137**, 121 (2000).
[2] E. Farhi and R. L. Jaffe, Phys. Rev. D **30**, 2379 (1984); E. Hiyama *et al.*, Prog. Theor. Phys. Suppl. **185**, 1 (2010).
[3] H. Takahashi *et al.*, Phys. Rev. Lett. **87**, 212502 (2001).
[4] C. J. Yoon *et al.*, Phys. Rev. C **75**, 022201 (2007).
[5] I. Wetzorke and F. Karsch, Nucl. Phys. B, Proc. Suppl. **119**, 278 (2003).
[6] Z. H. Luo, M. Loan, and X. Q. Luo, Mod. Phys. Lett. A **22**, 591 (2007).
[7] T. Inoue *et al.* (HAL QCD Collaboration), Prog. Theor. Phys. **124**, 591 (2010).
[8] S. R. Beane *et al.* (NPLQCD Collaboration), preceding Letter, Phys. Rev. Lett. **106**, 162001 (2011).
[9] N. Ishii, S. Aoki, and T. Hatsuda, Phys. Rev. Lett. **99**, 022001 (2007); H. Nemura, N. Ishii, S. Aoki, and T. Hatsuda, Phys. Lett. B **673**, 136 (2009); S. Aoki, T. Hatsuda, and N. Ishii, Prog. Theor. Phys. **123**, 89 (2010).
[10] Reviewed in M. Oka, K. Shimizu, and K. Yazaki, Prog. Theor. Phys. Suppl. **137**, 1 (2000); Y. Fujiwara, Y. Suzuki, and C. Nakamoto, Prog. Part. Nucl. Phys. **58**, 439 (2007).
[11] K. Murano, N. Ishii, S. Aoki, and T. Hatsuda, arXiv:1012.3814.
[12] M. Lüscher, Nucl. Phys. **B354**, 531 (1991); M. Fukugita *et al.*, Phys. Rev. D **52**, 3003 (1995).
[13] N. Ishii *et al.* (HAL QCD Collaboration) (to be published).
[14] T. Ishikawa *et al.* (CP-PACS and JLQCD Collaborations), Phys. Rev. D **78**, 011502 (2008); http://www.jldg.org/ildg-data/CPPACS+JLQCDconfig.html
[15] See S. Aoki *et al.* (PACS-CS Collaboration), Phys. Rev. D **79**, 034503 (2009) for details of the DDHMC/PHMC code.
[16] N. Ishii (PACS-CS and HAL QCD Collaborations), Proc. Sci., LAT2009 (2009) 019 [arXiv:1004.0405].
[17] K. Sasaki (HAL QCD Collaboration), Proc. Sci., LAT2010 (2010) 157.
[18] Columbia Physics System (CPS), http://qcdoc.phys.columbia.edu/cps.html.
[19] Japan Lattice Data Grid, http://www.jldg.org; International Lattice Data Grid, http://www.lqcd.org/ildg.